CHILEAN JOURNAL of AGRICULTURAL RESEARCH
RESEARCH ARTICLE

Selection and characterization of rhizobacteria from cocoa soils in Ecuador with potential for cadmium mitigation

Hayron Canchignia Martínez[1, 2], Javier Auhing Arcos[1, 2*], Luis Vera Benites[1, 2], Wuellins Durango Cabanilla[3], Karina Peña Salazar[3], and Manuel Carrillo Zenteno[2, 3]

[1]Universidad Técnica Estatal de Quevedo (UTEQ), Facultad de Ciencias Agrarias y Forestales, Campus La María, Mocache, Los Ríos, Ecuador.
[2]Universidad Técnica Estatal de Quevedo (UTEQ), Unidad de Posgrado, Quevedo, Los Ríos, Ecuador.
[3]Instituto Nacional de Investigaciones Agropecuarias de Ecuador (INIAP), Estación Experimental Tropical Pichilingue (EETP), Departamento de Suelo y Agua, Mocache, Los Ríos, Ecuador.
*Corresponding author (javier.auhing@uteq.edu.ec).
Received: 4 May 2026; Accepted: 5 August 2026, Available online: 7 September 2026. doi:10.4067/S0718-58392026000600978

ABSTRACT

Bioprospecting for Cd-tolerant rhizobacteria that naturally inhabit cocoa (*Theobroma cacao* L.) soils contaminated with heavy metals contributes to the development of effective bioremediation strategies. The objective of this study was to select rhizobacteria from cocoa soils in Ecuador with the potential for Cd mitigation. Soil samples were collected from the provinces of Cañar, Esmeraldas, and Manabí. Morphological and biochemical characteristics, Cd tolerance, and molecular identification of the 16S rRNA gene were evaluated. Twelve rhizobacteria morphotypes were selected for their capacity to tolerate 50 mg Cd L^{-1} for 24 h while producing protease, catalase, and urease enzymes, biofilm production, and solubilizing phosphate and K. Autochthonous strains T-CADM-1, T-CADM-4, T-CADM-5, and T-CADM-6 were incubated at four Cd concentrations (0, 6, 12 and 24 mg L^{-1}) for 7 d, maintaining significant cell persistence ($p \leq 0.05$) of 2.06×10^9, 2.02×10^9, 2.08×10^9 and 1.96×10^9 CFU mL^{-1}, respectively. The strain T-CADM-5 was the most effective, precipitating bicarbonate (139%) and achieving an in vitro Cd removal rate of 82.4%. GenBank data identified the tolerant strains as *Enterobacter* sp. (86%), *Serratia marcescens* (98%), *E. asburiae* (92%) and *E. hormaechei* (98%). It was concluded that the strain T-CADM-5 retained its cell viability for 7 d under Cd stress, produced urease and phosphatase, and increased bicarbonate and sulfate anions. These factors positively correlated with Cd immobilization, indicating that these rhizobacteria actively modify their environment to reduce the bioavailability of the heavy metal.

Key words: Bioremediation, Cd-tolerant rhizobacteria, phosphate-solubilizing, *Theobroma cacao*, urease.

INTRODUCTION

Cadmium (Cd) is a toxic, mobile chalcophile that bioaccumulates at the soil-root interface, posing risks of renal and oncogenic pathologies. In Ecuador, soil Cd averages 0.44 mg kg^{-1}, yet peeled cocoa (*Theobroma cacao* L.) beans reach 0.9 mg kg^{-1}, with 45% of samples exceeding the 0.6 mg kg^{-1} regulatory threshold. This disparity results from high uptake in geologically young soils, necessitating amendments to lower metal bioavailability (Argüello et al., 2019). Cadmium-tolerant rhizobacteria (CdtrB) have emerged as a sustainable in situ bioremediation strategy to mitigate Cd within tropical agroecosystems. These agents drive sequestration through biosorption, intracellular bioaccumulation, and biomineralization, mediated by functional groups such as amide, carbonyl, and phosphate within the bacterial biomass (Bravo and Braissant, 2022).

The efficacy of CdtrB depends on ecological fitness and adaptation to site-specific edaphic constraints (Bravo et al., 2018). Genera such as *Acinetobacter*, *Bacillus*, *Pseudomonas*, *Enterobacter*, and *Serratia* have

demonstrated significant potential for Cd mitigation and express diverse plant growth-promoting rhizobacteria (PGPR) traits. Specifically, CdtrB strains producing urease and carbonic anhydrase facilitate the precipitation of bicarbonate (HCO_3^-) and carbonate (CO_3^{2-}), leading to microbially induced carbonate precipitation (MICP) and subsequent Cd immobilization (Bhattacharya et al., 2018; Ma et al., 2023). Furthermore, PGPR functional traits—including phosphate solubilization, siderophore synthesis, and proteolytic activity—mitigate abiotic and biotic stress (Pal and Sengupta, 2019; Canchignia-Martínez et al., 2024; Huang et al., 2026). Enhance crop resilience to abiotic stresses, including salinity and drought, by stimulating biomass accumulation and activating antioxidant defense pathways. Leveraging their proven capacity to mitigate environmentally induced cellular damage, PGPR present a compelling biotechnological strategy for alleviating heavy metal toxicity in agricultural systems (Chompa et al., 2024; Stamenov et al., 2024). Consequently, the inoculation of CdtrB with PGPR functional traits has emerged as a promising strategy for the in situ immobilization and detoxification of heavy metals in contaminated soils (Abdollahi et al., 2020). This study aims to select rhizobacteria from high-Cd soils in the provinces of Cañar, Esmeraldas, and Manabí, Ecuador, to evaluate the effectiveness of CdtrB in reducing bioavailable Cd concentrations.

MATERIALS AND METHODS

Agroclimatic and edaphic variability of the study sites

Composite soil samples (1 kg) were collected in 2022 from commercial *Theobroma cacao* L. plantations in the Ecuadorian provinces of Manabí, Cañar, and Esmeraldas, using a systematic random design with 10 sub-samples per site, sampled sites were georeferenced using WGS84 Datum/UTM zone 17 into South America Equidistant Conic coordinate system – Environmental Systems Research Institute (ESRI): 102032 (Table 1). After removing the superficial organic horizon, the rhizospheric soil (0-10 cm) was homogenized in situ and transported in sterile high-density polyethylene bags. Particle size distribution was determined in triplicate using the Bouyoucos hydrometer method, with sodium hexametaphosphate as the dispersing agent. Simultaneously, the agroclimatic profile of the localities was structured based on historical series (2013-2023) of mean annual precipitation, temperature, and relative humidity obtained from local meteorological stations and regional databases (Table 1).

Table 1. Geographic, edaphic, and agroclimatic parameters of the sampling zones (2013-2023 average). *Value reported according to Instituto Nacional de Meteorología e Hidrología (INAMHI) database (Quito, Ecuador). RH: Relative humidity.

Location	UTM			Above sea level	Texture	Topography	Temperature*	Rainfall*	RH*
	X	Y	Band	m			°C	mm	%
Canuto (Manabí)	598287.29	9911565.33	S	150	Clay loam	flat	28.0	1250	78.2
La Troncal (Cañar)	684609.15	9732034.13	S	82	Silty clay loam	regular	24.6	2000	88.0
San Lorenzo (Esmeraldas)	740907.67	142256.36	N	14	Silty clay	flat	29.8	2947	30.4

Chemical and microbiological characteristics of soils

Determination of soil semi-total Cd. Samples were dried at 27 °C and sieved at 2 mm. Soil samples (50 mg) were digested in boiling aqua regia (1:3 Suprapur HCl:HNO_3), $HClO_4$ (2 mL) and HNO_3 (8 mL) (Argüello et al., 2019), with a 1 h resting period followed by heating at 180 °C for 90 min until extract clarification and emission of white vapor. After filtration and dilution to 50 mL with ultrapure water, for at least 4 h and the elemental composition of the digest was determined by Graphite Furnace Atomic Absorption Spectrometry (AAnalyst 400, PerkinElmer, Shelton, Connecticut, USA) at 228.8 nm, detection limit: 1.21 µg kg^{-1} Cd, quantification limit: 4.04 µg kg^{-1} Cd, with results expressed in mg kg^{-1}. Using RStudio (Posit Software, PBC, Boston, Massachusetts, USA), the spatial distribution of Cd (log-transformed) was modeled using log-normal kriging and exponential semivariograms. The interpolation results were overlaid onto the agricultural geoportal of Ecuadorian government official zoning map. Because sampling was only conducted on cacao plantations, the map is not representative for other land uses.

Determination of bacterial load in cocoa soils. One gram of moist soil was suspended in 99 mL sterile distilled water and 10 µL was recovered and diluted in 90 µL sterile distilled water. Serial dilutions (up to 10^{-8}) were made and incubated in a nutritive agar medium. The microdrop technique was used for the formation of rhizobacteria colonies, which were incubated for 48 h at 28 °C (Lee et al., 2021). Colonies were counted, and the results were expressed as colony-forming units (CFU) per gram of soil:

$$CFU\ g^{-1} = [(N/V_S) \times (1/D) \times (V_0/m)] \quad (1)$$

where N is the average number of colonies counted per microdrop, V_S is the volume of the microdrop plated (mL), D is the serial dilution from which the count was made, V_0 is the total volume of the initial soil suspension (mL), and m is the equivalent dry mass of the initial soil sample (g).

Isolation of Cd-tolerant rhizobacteria

Ten grams of composite sample from the rhizosphere of each cocoa-based cropping system studied were introduced into an Erlenmeyer flask containing 90 mL sterile distilled water (Ntsoli et al., 2025), with a concentration of 50 mg L^{-1} Cd (atomic absorption standard AA08N-5) and shaken in the dark in a shaker (Orbital shaker DOS-20L, ELMI, Riga, Municipality, Latvia) for 48 h at 50 rpm. A volume of 100 µL was recovered and cultivated on King B agar (g L^{-1}): Peptone (20); glycerol (15), K_2HPO_4 (1.5), $MgSO_4 \cdot 7H_2O$, (1.5), agar, (15) at a concentration of 50 mg L^{-1} Cd, in plates incubated at 27 °C for 48 h. To distinguish and choose the Cd-tolerant rhizobacterial colonies, fluorescent pigmentation was recorded on King B Agar under ultraviolet light (365 nm) (Canchignia-Martínez et al., 2024). Colonies positive for fluorescence were selected under a UV light lamp, and the strains were purified and cryopreserved in a 30% (v/v) glycerol solution at -80 °C.

Morphological and biochemical characterization

Their macroscopic morphology was described based on shape (circular, punctiform, irregular, or spindle-shaped), margin (entire, undulated, lobed, or filamentous), and elevation (flat, convex, or raised). The microscopical identification was carried out by Gram staining. The process of Gram staining was carried out by making rhizobacterial smears on the glass of objects, followed by adding violet crystal, mordant, alcohol, and safranin. A screening of biochemical characteristics was performed in three replicates using the qualitative method to evaluate the rhizobacteria strains. The data obtained were subjected to a cluster analysis using Centurion XVI (Statgraphics Technologies, The Plains, Virginia, USA). *Pseudomonas protegens* CHA0 and *Serratia marcescens* PM3-8 (Chávez-Arteaga et al., 2018), positive for plant growth promoting rhizobacteria (PGPR), were used as control rhizobacteria.

Antibiogram of Cd-tolerant rhizobacteria. Antibiotic susceptibility was evaluated using the Kirby-Bauer disk diffusion method. Briefly, rhizobacteria were cultured on King B agar (15 g L^{-1}). Within 15 min of inoculation, 5-mm diameter disks impregnated with either ampicillin (500 mg L^{-1}) or chloramphenicol (500 mg L^{-1}) were applied to the agar surface. Following a 24 h incubation at 37 °C, susceptibility was assessed by observing the corresponding zones of growth inhibition (Adkin et al., 2022).

Identification of proteolytic and catalase activity. Proteolytic activity was evaluated by inoculating 20 µL liquid culture (King B, 24 h, 27 °C, 200 rpm) into gelatin medium (g L^{-1}): Peptone (4), yeast extract (1), gelatin (12), agar (15). Degradation halos were recorded after 24 h. The catalase test was performed by detecting effervescence following the addition of hydrogen peroxide (H_2O_2) (Chávez-Arteaga et al., 2018).

Evaluation of enzymatic activity and solubilization. Rhizobacteria were incubated in 75 mL liquid King B medium (28 °C, 24 h, 180 rpm). Aliquots of 5 µL cell suspension were inoculated into tubes with specific media. Christensen's urea agar (ureolytic activity) (g L^{-1}): Peptone (1), dextrose (1), NaCl (5), K_2HPO_4 (2), urea (20), phenol red (0.012), agar (15). National Botanical Research Institute of Phosphate (NBRIP) broth (phosphate solubilization) (g L^{-1}): Glucose (10), $Ca_3(PO_4)_2$ (5), $MgCl_2 \cdot 6H_2O$ (5), $MgSO_4 \cdot 7H_2O$ (0.25), KCl (0.2), $(NH_4)_2SO_4$ (0.1) (Park et al., 2011). Modified Pikovskaya agar (K solubilization) (g L^{-1}): Glucose (10), KNO_3 (5), KCl (0.2), $(NH_4)_2SO_4$ (0.5), $MgSO_4 \cdot 7H_2O$ (0.1), bromocresol purple (0.125), agar (15) (Canchignia-Martínez et al., 2024); and incubated at 28 °C for 3 d. The process was repeated in triplicate. Solubility was visually assessed 72 h after inoculation. Each colony exhibiting a clear halo zone was observed.

Biofilm production. Biofilm formation was estimated using the crystal violet (CV) staining technique. The Cd-tolerant rhizobacteria (CdtrB) strains were cultured in 10 mL dextrose-peptone-yeast broth (g L^{-1}): Glucose (20), yeast extract (10), casein peptone (10) at 29 ± 1 °C for 24 h. After rinsing with phosphate buffered saline (PBS), matrices were stained with 1% CV for 20 min. Finally, tubes were washed with distilled water, and biofilm formation was confirmed by the presence of a pigmented ring at the air-liquid interface (Koua et al., 2020).

Determination of rhizobacterial persistence under Cd stress

The selection of autochthonous rhizobacteria with Cd tolerance (from Cañar, Esmeraldas, and Manabí) was determined by assessing the minimum inhibitory concentration (MIC), defined as the lowest Cd concentration that completely suppresses visible rhizobacterial growth (Adkin et al., 2022). The evaluation was conducted in liquid M9 minimal medium (g L^{-1}): Na_2HPO_4 (5.8), KH_2PO_4 (3), NaCl (0.5), NH_4Cl (1), glucose (2), $MgSO_4 \cdot 7H_2O$ (0.49), $CaCl_2 \cdot 2H_2O$ (0.015), thiamine (0.010), pH 6.5 (Peñafiel et al., 2016; Azatian et al., 2019); adding increasing concentrations of Cd (0, 6, 12, and 24 mg L^{-1}). Cultures were incubated at 28 °C and 180 rpm. After 7 d, population density (CFU mL^{-1}) was quantified using the surface microdrop plate count method (Nasser et al., 2024). Colony-forming units were calculated using the following equation:

$$CFU\ mL^{-1} = (\text{Number of colonies/Dispensed volume in } mL^{-1}) \times \text{Dilution factor}] \quad (2)$$

Determination of bicarbonate (HCO_3^-) levels in the growth medium under Cd stress

The HCO_3^- concentration was determined by the potentiometric titration with sulfuric acid 0.025 M (H_2SO_4), following AOAC 920.194 analytical protocol (Carbonate and Bicarbonate in Water/Titrimetric Method), the data are expressed in mg L^{-1}. This derived from rhizobacterial metabolic activity in response to concentrations of Cd stress. The dynamics of this anion were evaluated by calculating its percentage increase:

$$\text{Increase (\%)} = [(Vf - Vi)/(Vi) \times 100] \quad (3)$$

where Vi and Vf represent the initial value (value before the increase) and final value (value after the increase), respectively, in mg L^{-1} (Andersen, 2019).

Determination of sulfate (SO_4^{2-}) levels in the growth medium under Cd stress

The SO_4^{2-} concentration was determined by spectrophotometry, using the standard method SM 4500-SO_4 E (Standard Methods for the Examination of Water and Wastewater), the data are expressed in mg L^{-1} (Sheikhi et al., 2020). This derived from rhizobacterial metabolic activity in response to concentrations of Cd stress. The dynamics of this anion were determined by calculating the percentage increase according to Equation 3.

Cd immobilization efficiency in the growth medium

The culture media of the treatments were centrifuged (BOECO C-28A) at 1300 rpm for 10 min to separate the biomass, and the resulting supernatant was quantified to determine the remaining Cd concentration at 228.8 nm using flame atomic absorption spectrometry (FAAS) with a AAnalyst 400 instrument (PerkinElmer) (Renu et al., 2022), the data are expressed in mg L^{-1}. The removal efficiency of the rhizobacteria was expressed via the immobilization index, calculated according to:

$$\text{Immobilization index (\%)} = [(Ci - Cf)/(Ci) \times 100] \quad (4)$$

where Ci and Cf represent the initial and final concentrations of heavy metals (mg L^{-1}), respectively (Wang et al., 2020).

Experimental design

A completely randomized design (CRD) was applied to determine the levels of Cd tolerance (cell viability) and the concentration of HCO_3^-, SO_4^{2-} and Cd in the growth medium. Thirteen treatments were used at different Cd concentrations (0, 6, 12 and 24 mg L^{-1}), and the absolute control. It was carried out under in vitro conditions, with three replicates per treatment. All data were subject to ANOVA, and the means were separated by Tukey's multiple range test ($p \leq 0.05$), using Centurion XVI (Statgraphics).

Pearson correlation analysis

This statistical approach evaluated the degree of linear association between cell viability (expressed as population density in CFU mL^{-1}), metabolic activity biomarkers (percentage increases of HCO_3^- and SO_4^{2-} anions), and overall system efficiency (Cd immobilization index). The magnitude and direction of these ecosystemic interactions were quantified via the correlation coefficient (r), establishing a highly stringent statistical significance level of $p < 0.001$.

Phylogenetic analysis based on the 16S rRNA gene

The nearly full-length 16S rRNA gene of strain CdtrB selected, the biomass recovered by centrifugation (10 000 × g for 1 min) was used for genomic DNA extraction using the UltraClean Microbial DNA Isolation kit (MO BIO, Carlsbad, California, USA). For the amplification of the 16S rRNA was PCR-amplified with primers 8F (5'-AGAGTTTGATCCTGGCTCAG-3') and 1492R (5'-ACGGCTACCTTGTTACGACTT-3'). The thermal profile consisted of an initial denaturation at 95 °C for 5 min, followed by 35 cycles of 95 °C for 45 s, annealing at 55 °C for 45 s, and extension at 72 °C for 2 min, with a final extension at 72 °C for 10 min (Chávez-Arteaga et al., 2018). The resulting amplicons (1500 bp) were purified using the PureLink kit (Invitrogen, Carlsbad, California, USA) and sequenced (Macrogen, Seoul, South Korea) using the internal primers 518F (5´-CCAGCAGCCGCGGTAATAC-´3) and 800R (3´-TACCAGGGTATCTAATCC-´5). Sequences were compared against the GenBank (NCBI) database using the BLAST tool. Multiple sequence alignment and phylogenetic tree topology were reconstructed using the Neighbor Joining method with 1000 bootstrap replicates. The Kimura 2-parameter (K2P) evolutionary model was selected based on the Bayesian Information Criterion (BIC) using MEGA 6.06 (Molecular Evolutionary Genetics Analysis) software (Sudhir Kumar, Koichiro Tamura, and Masatoshi Nei, Tempe, Arizona, USA, and Tokyo, Japan).

RESULTS AND DISCUSSION

Agroclimatic and edaphic variability of the study sites

The sampling sites exhibited a contrasting climatic and edaphic gradient across the coastal region and the Andean foothills (Table 1). These variations delineate distinct environments that govern Cd dynamics and the associated microbiota, indicating the robust ability of the strains to sense and respond to environmental changes (Huang et al., 2026).

Special analysis of semi-total Cd and bacterial load in cocoa soils in Ecuador

The geospatial distribution of soil Cd concentrations across the sampled regions in Ecuador reveals significant spatial heterogeneity, with values ranging from 0.63 to 0.95 mg kg^{-1}. The highest Cd accumulation was identified at the San Lorenzo sampling site (Esmeraldas) at 0.95 mg kg^{-1}, followed by Canuto (Manabí) and La Troncal (Cañar) with concentrations of 0.75 and 0.63 mg kg^{-1}, respectively (Figure 1). The heatmap highlights distinct hotspots in the northern and coastal agricultural belts, suggesting a concentration gradient that may necessitate site-specific bioremediation strategies to ensure edaphic resilience and food safety in cocoa-growing soils (Argüello et al., 2019).

The dual-axis plot illustrates the negative correlation between semi-total Cd levels (mg kg^{-1}) and the bacterial counts (CFU g^{-1}) (Figure 2). Soils from the Esmeraldas province, which exhibited the highest metal enrichment (0.95 mg kg^{-1}), supported the lowest bacterial density at 4.26×10^5 CFU g^{-1}. In contrast, the control soil—characterized by undetectable Cd levels—harbored a significantly more robust microbial population of 1.66×10^6 CFU g^{-1}. These results indicate that increasing Cd bioavailability exerts a pronounced inhibitory pressure on soil microbiota, suggesting that heavy metal toxicity is a primary driver of reduced biological activity in these cocoa-growing regions (Pal and Sengupta, 2019). In this context, the isolation of rhizobacteria strains with specific Cd tolerance mechanisms in anthropogenically impacted environments has been previously documented (Bravo et al., 2018; Bravo and Braissant, 2022).

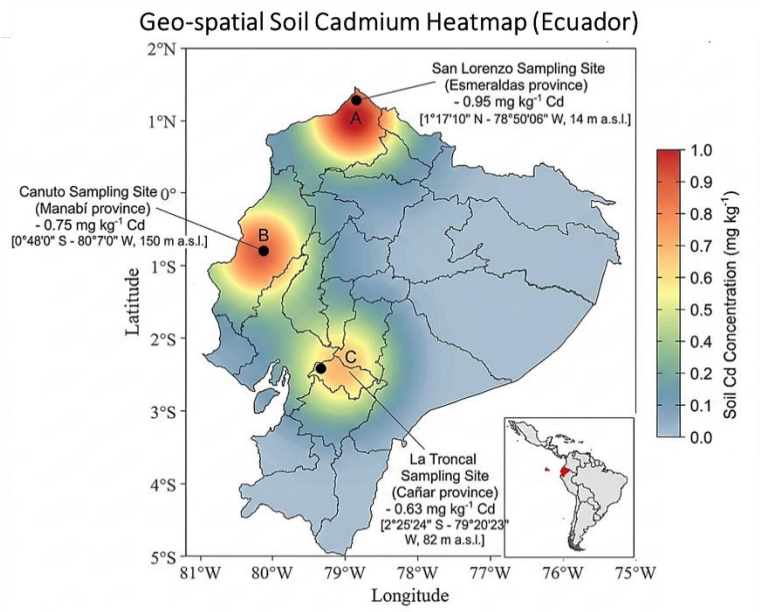

Figure 1. Geospatial soil Cd concentrations across selected agricultural provinces in Ecuador. The colorimetric scale indicates total soil Cd levels ranging from 0.0 to 1.0 mg kg^{-1}. The map shows the geographical location of the study area within South America.

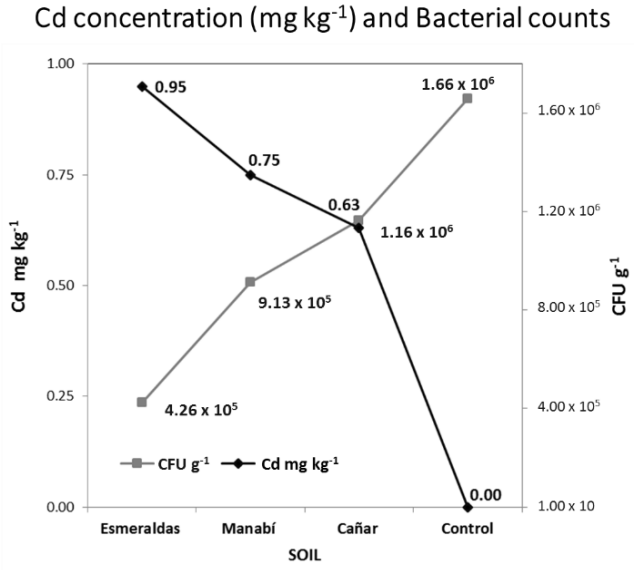

Figure 2. Monitoring of soils in Ecuador with a history of Cd. Concentration of Cd levels and bacterial counts in soil samples contaminated with heavy metals and without contamination (Control). CFU: Colony forming units.

Morphological and biochemical characterization

From 30 rhizobacteria isolates obtained from soils of cacao rhizosphere (Table 2), with tolerance to 50 mg L^{-1} Cd, twelve strains with fluorescence emission characteristics were selected due to their similarity to the positive controls *Pseudomonas protegens* CHA0 and *Serratia marcescens* PM3-8, both identified as plant growth-promoting rhizobacteria (PGPR) (Chávez-Arteaga et al., 2018).

Table 2. Cadmium-tolerant rhizobacteria collected from Ecuadorian cacao soils.

Province	Canton	Amount of rhizobacteria	Strains
Manabí	Canuto	10	T-CADM-1, T-CADM-2, T-CADM-3, T-CADM-4, T-CADM-5, T-CADM-6, T-CADM-7, T-CADM-8, T-CADM-9, T-CADM-10
Cañar	La Troncal	10	T-CADTC-1, T-CADTC-2, T-CADTC-3, T-CADTC-4, T-CADTC-5, T-CADTC-6, T-CADTC-7, T-CADTC-8, T-CADTC-9, T-CADTC-10
Esmeraldas	San Lorenzo	10	T-CADE-1, T-CADE-2, T-CADE-3, T-CADE-4, T-CADE-5, T-CADE-6, T-CADE-7, T-CADE-8, T-CADE-9, T-CADE-10

Morphological and biochemical analysis of Cd-tolerant rhizobacteria (CdtrB) reveals a remarkable adaptability and potential for Cd mitigation in cocoa soils. The selected rhizobacteria demonstrated high Cd tolerance, up to 50 mg L^{-1} (Table 3). Morphological divergence was evident between the T-CADM (Manabí) series, which exhibited predominantly Gram-negative, circular colonies, and the T-CADTC (Cañar) and T-CADE (Esmeraldas) cohorts, characterized by punctiform, flat morphologies and frequent Gram-positive reactions. A distinct functional dichotomy emerged regarding nutrient solubilization: The T-CADTC (Cañar) and T-CADE (Esmeraldas) series demonstrated superior K solubilization, whereas the T-CADM group occupied a specialized niche defined by conserved P solubilization and high ureolytic activity (Figures 3A and 3B). Ureolytic activity hydrolyzes urea [$CO(NH_2)_2$] to produce ammonia, which sequentially reacts with carbonic acid to generate HCO_3^- and carbonate CO_3^{2-} anions (Bhattacharya et al., 2018).

Table 3. Morphological and biochemical characterization profile of the Cd-tolerant rhizobacteria. U: Undulate; E: entire; Cv: convex; Pl: flat; P: punctiform; C: circular. N: negative; P: positive; higher presence: (++); presence: (+); absence: (-); R: resistant; S: susceptible.

	Morphological					Biochemical							
Strain	Edge shape	Height	Form of colony	Gram stain	Fluorescence	Solubilization of K	Solubilization of P	Urease	Protease	Biofilm	Catalase	Chloramphenicol	Ampicillin
T-CADM-1	E	Cv	C	N	+	-	+	+	+	+	+	S	R
T-CADM-4	E	Cv	C	N	+	-	+	+	-	-	+	R	R
T-CADM-5	U	Cv	C	N	+	-	+	+	-	-	+	S	S
T-CADM-6	E	Cv	C	N	+	-	++	+	+	+	+	S	R
T-CADTC-3	U	Pl	P	P	+	++	-	-	-	-	+	R	R
T-CADTC-4	U	Pl	P	P	+	++	-	-	-	-	+	R	R
T-CADTC-5	U	Pl	P	P	+	++	-	+	+	-	+	R	R
T-CADTC-8	U	Pl	P	N	+	++	-	+	-	-	+	R	R
T-CADE-2	U	Pl	P	P	+	++	-	++	-	-	+	R	R
T-CADE-3	U	Pl	P	P	+	++	-	+	-	-	+	R	R
T-CADE-7	U	Pl	P	N	+	++	-	+	-	-	+	R	R
T-CADE-10	U	Pl	C	N	+	-	++	++	+	-	+	R	R
P. protegens CHA0	E	Pl	C	N	+	+	+	++	+	+	+	R	R
S. marcescens PM3-8	E	Cv	C	N	++	+	++	++	++	+	+	R	R

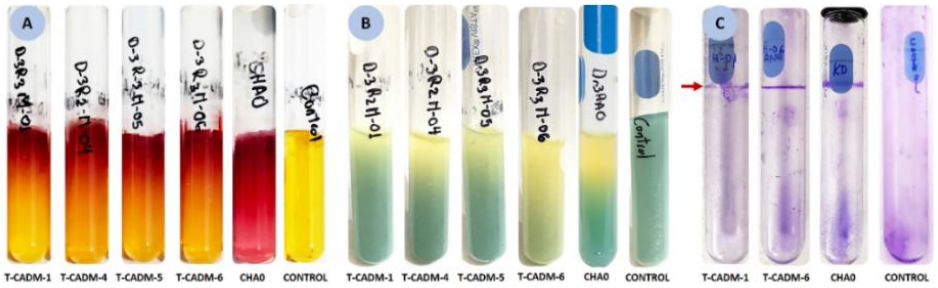

Figure 3. Biochemical characterization of Cd-tolerant rhizobacteria: Urease-positive rhizobacteria developed red color (A); activity of acid phosphatase in strains grown in NBRIP (B); biofilm production, i.e. solid biofilms associated to the rhizobacteria surface, deemed positive when a ring was formed in the tube (C). NBRIP: National Botanical Research Institute of Phosphate broth (phosphate solubilization).

This isolates T-CADM-1 and T-CADM-6, exhibited biofilm-forming capacities (Figure 3C), matching reference strains *P. protegens* CHA0 and *S. marcescens* PM3-8. The resulting biofilm matrix functions as a sacrificial electrostatic shield and diffusion barrier, safeguarding cellular integrity and preserving membrane homeostasis against heavy-metal-induced oxidative stress (Gupta and Diwan, 2017). Among these mechanisms, the ability to produce low molecular weight organic acids stands out, which are fundamental in the solubilization of soil phosphate, increase its nutritional availability to plants (Chen et al., 2021).

In addition, siderophore-mediated fluorescence (which indicates the presence of pioverdine-type siderophores) and proteolytic enzymes like protease (PR) (Figures 4A and 4B) suggest increased metabolic activity and structural protection of the rhizosphere against plant pathogens (Bensidhoum et al., 2016; Peñafiel et al., 2016). From an evolutionary perspective, intrinsic antimicrobial resistance (Figure 4C) to ampicillin and chloramphenicol across most isolates—save for the susceptible T-CADM-5—evidences a prevalent co-selection phenomenon linking heavy metal tolerance with antimicrobial resilience. Tolerances to antibiotics and heavy metals may help rhizobacteria to adapt themselves to conditions of heavy metal stress faster by the expansion of resistant factors than by mutation and natural selection (Abdollahi et al., 2020).

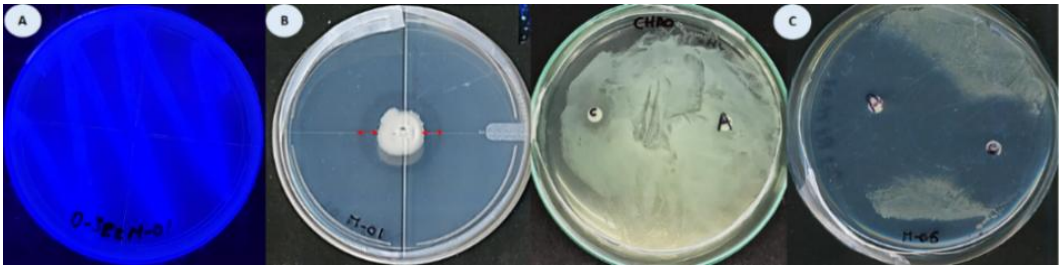

Figure 4. Screening of Cd-tolerant rhizobacteria with plant growth-promoting rhizobacteria functional traits: Rhizobacteria strain with fluorescent pigmentation (A); proteolytic activity (B) (arrow points to the degradation halo around the colony on gelatin agar medium); antimicrobial resistance (C). A: Ampicillin; C: chloramphenicol.

Cluster analysis of CdtrB isolates. Cluster analysis based on the morphological and biochemical characteristics of CdtrB isolated from cocoa soils in Ecuador has revealed two main groups (Figure 5). Group A, englobes rhizobacteria from Manabí (T-CADM-1, T-CADM-4, T-CADM-5, T-CADM-6), a strain from Esmeraldas (T-CADE-10), and the positive controls *P. protegens* CHA0 and *S. marcescens* PM3-8, suggesting their potential as PGPR and the synergistic integration of specialized enzymatic machinery, such as ureolytic potential, and robust metal-stress resilience (Pal and Sengupta, 2019).

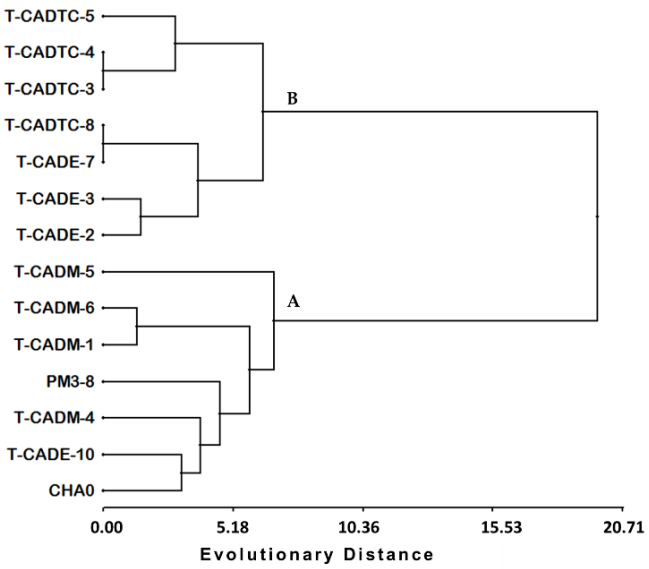

Figure 5. Cluster analysis of the morphological and biochemical traits of Cd-tolerant rhizobacteria isolates. Evolutionary distance was deduced using the Euclidean method. The phylogenetic tree was constructed using Ward's method.

Determination of rhizobacterial persistence under Cd stress

All autochthonous rhizobacteria exhibited high cellular persistence across the Cd gradient, maintaining populations above 10^7 CFU mL^{-1} after 7 d of incubation (Table 4). Notably, T-CADM-1 and T-CADTC-5 achieved their maximum growth ($p \leq 0.05$) under acute toxicity (24 mg L^{-1}), reaching 2.80×10^9 and 2.78×10^9 CFU mL^{-1}, respectively. In contrast, the reference strain *P. protegens* CHA0 showed a significant decline in density at the highest metal concentration (1.46×10^9 CFU mL^{-1}) compared to its performance under moderate stress. This robust survival suggests that the autochthonous strains possess superior adaptive mechanisms—such as efficient metal efflux systems or extracellular sequestration—allowing them to remain metabolically active under severe Cd stress (Das et al., 2016; Bravo and Braissant, 2022). Such persistence is a prerequisite for effective assisted bioremediation, as it ensures the stability of the microbial population required to drive the biomineralization of heavy metals in contaminated soils (Bravo et al., 2018; Feria-Cáceres et al., 2022).

Table 4. Cellular persistence of autochthonous rhizobacteria across increasing Cd concentrations after 7 d of incubation. Means followed by similar letters do not show significant differences ($p \leq 0.05$) according to Tukey's multiple comparison test. CFU: Colony forming units.

Treatments	Concentration of Cd (mg L^{-1})				Mean CFU mL^{-1}
	0	6	12	24	
T-CADM-1	1.61×10^{9ab}	1.68×10^{9ab}	2.17×10^{9ab}	2.80×10^{9a}	2.06×10^9
T-CADM-4	2.12×10^{9a}	2.03×10^{9ab}	1.48×10^{9ab}	2.45×10^{9abc}	2.02×10^9
T-CADM-5	1.58×10^{9ab}	2.28×10^{9ab}	2.11×10^{9ab}	2.36×10^{9abcd}	2.08×10^9
T-CADM-6	1.57×10^{9ab}	2.57×10^{9a}	2.18×10^{9ab}	1.54×10^{9bcd}	1.96×10^9
T-CADTC-3	2.80×10^{8bc}	2.15×10^{9ab}	2.46×10^{9ab}	1.40×10^{9cd}	1.57×10^9
T-CADTC-4	2.49×10^{8bc}	2.01×10^{9ab}	2.60×10^{9a}	2.55×10^{9abc}	1.85×10^9
T-CADTC-5	1.01×10^{9abc}	1.14×10^{9b}	8.40×10^{8b}	2.78×10^{9a}	1.44×10^9
T-CADTC-8	1.66×10^{9ab}	1.13×10^{9b}	2.00×10^{9ab}	2.60×10^{9abc}	1.85×10^9
T-CADE-2	5.79×10^{8bc}	1.87×10^{9ab}	1.17×10^{9ab}	1.76×10^{9abcd}	1.34×10^9
T-CADE-3	7.38×10^{8abc}	1.07×10^{9b}	1.17×10^{9ab}	1.16×10^{9d}	1.04×10^9
T-CADE-7	1.27×10^{9abc}	1.85×10^{9ab}	1.39×10^{9ab}	2.69×10^{9ab}	1.80×10^9
T-CADE-10	2.54×10^{7c}	2.35×10^{9ab}	2.08×10^{9ab}	2.53×10^{9abc}	1.75×10^9
CHA0	2.15×10^{9a}	2.64×10^{9a}	1.71×10^{9ab}	1.46×10^{9cd}	1.99×10^9

Dynamics of bicarbonate (HCO_3^-) levels in the growth medium under Cd stress

All rhizobacteria treatments significantly increased ($p \leq 0.05$) HCO_3^- production (Table 5) compared to the uninoculated control across all Cd concentrations. In the absence of metal stress, T-CADM-5 achieved the highest HCO_3^- levels (101.1 mg L^{-1}), representing a 139.1% increase over the control. Under acute toxicity (24 mg Cd L^{-1}), T-CADM-5 and T-CADM-6 maintained superior metabolic activity, reaching 99.86 and 99.92 mg L^{-1}, respectively, which was statistically comparable to the reference strain CHA0 (97.98 mg L^{-1}). This robust HCO_3^- generation suggests highly active ureolytic pathways within these autochthonous isolates (Ma et al., 2023). In the context of agricultural bioremediation, the microbially induced precipitation of HCO_3^- and CO_3^{2-} serves as a primary mechanism for immobilizing Cd, effectively converting the bioavailable heavy metal into stable, insoluble complexes within the soil matrix (Dhami et al., 2016; Giri and Pant, 2019; Bravo and Braissant, 2022).

Table 5. Bicarbonate (HCO_3^-) precipitation and percentage increase driven by autochthonous rhizobacteria across different Cd concentrations, after 7 d of incubation. Values are mean ± SD (n = 3). Means with similar letters within the same column do not show statistically significant differences ($p \leq 0.05$) by Tukey's multiple comparison test.

Treatments	Concentration of Cd (mg L^{-1})				% Increase HCO_3^-
	0	6	12	24	
T-CADM-1	96.09 ± 9.47^{ab}	91.52 ± 19.44^{a}	94.99 ±1 9.91^{ab}	92.98 ± 1.42^{abc}	119.60
T-CADM-4	95.63 ± 8.21^{ab}	94.91 ± 14.99^{a}	82.00 ± 2.80^{ab}	75.92 ± 2.48^{cd}	103.70
T-CADM-5	101.10 ± 8.95^{a}	99.83 ± 16.74^{a}	108.20 ± 10.69^{a}	99.86 ± 0.14^{a}	139.10
T-CADM-6	95.81 ± 9.45^{ab}	91.00 ± 13.33^{a}	93.80 ± 3.40^{ab}	99.92 ± 1.28^{a}	122.50
T-CADTC-3	81.33 ± 6.12^{abc}	80.88 ± 9.78^{a}	82.29 ± 4.95^{ab}	77.27 ± 6.10^{bcd}	88.10
T-CADTC-4	88.00 ± 8.38^{abc}	85.79 ± 5.70^{a}	88.60 ± 5.80^{ab}	86.59 ± 11.07^{abcd}	104.00
T-CADTC-5	67.97 ± 4.81^{cd}	80.61 ± 12.49^{a}	73.95 ± 7.03^{b}	71.60 ± 13.69^{d}	71.95
T-CADTC-8	73.72 ± 13.62^{bcd}	71.45 ± 7.42^{ab}	74.56 ± 14.32^{b}	71.53 ± 9.55^{d}	70.27
T-CADE-2	72.83 ± 6.02^{bcd}	75.85 ± 4.73^{a}	82.07 ± 3.76^{ab}	76.92 ± 7.17^{bcd}	79.86
T-CADE-3	87.99 ± 2.79^{abc}	83.61 ± 7.33^{a}	86.12 ± 3.11^{ab}	89.95 ± 6.34^{abcd}	103.20
T-CADE-7	88.57 ± 9.66^{abc}	87.40 ± 4.50^{a}	97.11 ± 10.64^{ab}	89.26 ± 6.34^{abcd}	111.80
T-CADE-10	94.59 ± 9.96^{ab}	88.67 ± 8.45^{a}	84.76 ± 13.21^{ab}	96.00 ± 4.00^{ab}	112.80
CHA0	89.69 ± 15.97^{abc}	99.45 ± 15.48^{a}	89.20 ± 6.80^{ab}	97.98 ± 5.18^{a}	119.90
Control without bacteria	51.85 ± 3.56^{d}	39.27 ± 3.19^{b}	40.41 ± 4.63^{c}	39.53 ± 3.52^{e}	0.00

Dynamics of sulfate (SO_4^{2-}) levels in the growth medium under Cd stress

The SO_4^{2-} production was significantly higher ($P \leq 0.05$) in all rhizobacteria treatments compared to the uninoculated control across the entire Cd gradient (Table 6). In the absence of metal stress, T-CADM-4 exhibited the highest basal production (3.85 mg L^{-1}), whereas under acute toxicity (24 mg L^{-1}), T-CADE-10 and the reference strain CHA0 achieved peak levels of 3.93 mg L^{-1}, representing a percentage increase of 131.4% and 144.4%, respectively. Sustained SO_4^{2-} flow under severe Cd stress indicates a robust S-oxidizing metabolism (Ultanbekova et al., 2025). These S-oxidizing bacteria (SOB) utilize multi-enzymatic systems to convert reduced sulfur into absorbable SO_4^{2-}, a critical oxidation process primarily driven by microbial biomass activity in agricultural soils (Ranadev et al., 2023), which is available to plants in the soil solution (Rana et al., 2020).

Table 6. Sulfate (SO_4^{2-}) production and percentage increase driven by autochthonous rhizobacteria across different Cd concentrations after 7 d of incubation. Values are mean ± SD (n = 3). Means with similar letters within the same column do not show statistically significant differences ($p \leq 0.05$) by Tukey's multiple comparison test.

	Concentration of Cd (mg L^{-1})				
Treatments	0	6	12	24	% Increase SO_4^{2-}
T-CADM-1	3.32 ± 0.80^{a}	2.78 ± 0.53^{a}	2.69 ± 0.58^{ab}	3.11 ± 0.05^{ab}	103.1
T-CADM-4	3.85 ± 0.10^{a}	3.08 ± 0.54^{a}	3.22 ± 1.00^{a}	3.11 ± 0.96^{ab}	126.3
T-CADM-5	3.43 ± 0.14^{a}	2.90 ± 0.11^{a}	3.78 ± 0.46^{a}	3.36 ± 1.04^{a}	129.9
T-CADM-6	3.00 ± 0.77^{a}	2.38 ± 0.36^{a}	3.80 ± 0.48^{a}	3.60 ± 0.39^{a}	118.1
T-CADTC-3	3.51 ± 0.59^{a}	2.95 ± 0.08^{a}	3.26 ± 0.26^{a}	3.75 ± 0.48^{a}	129.9
T-CADTC-4	3.69 ± 0.50^{a}	2.93 ± 0.12^{a}	3.30 ± 0.54^{a}	3.13 ± 0.98^{ab}	122.7
T-CADTC-5	3.49 ± 0.24^{a}	3.18 ± 0.57^{a}	2.74 ± 0.41^{ab}	3.00 ± 0.37^{ab}	111.8
T-CADTC-8	2.70 ± 0.16^{a}	2.73 ± 0.08^{a}	2.62 ± 0.47^{ab}	3.41 ± 0.38^{a}	95.56
T-CADE-2	3.26 ± 0.15^{a}	2.67 ± 0.54^{a}	2.87 ± 0.69^{ab}	3.07 ± 0.59^{ab}	102.6
T-CADE-3	3.09 ± 0.32^{a}	2.75 ± 0.26^{a}	2.89 ± 0.58^{ab}	3.69 ± 0.29^{a}	111.9
T-CADE-7	3.72 ± 0.16^{a}	3.09 ± 0.16^{a}	2.97 ± 0.51^{ab}	3.46 ± 0.56^{a}	125.9
T-CADE-10	3.73 ± 0.30^{a}	3.19 ± 0.17^{a}	2.71 ± 0.32^{ab}	3.93 ± 0.19^{a}	131.4
CHA0	3.03 ± 0.26^{a}	3.31 ± 0.17^{a}	4.05 ± 0.13^{a}	3.93 ± 0.07^{a}	144.4
Control without bacteria	1.40 ± 0.46^{b}	1.33 ± 0.43^{b}	1.55 ± 0.43^{b}	1.58 ± 0.79^{b}	0.00

Cd immobilization efficiency in the growth medium

The rhizobacteria exhibited highly significant ($P \leq 0.05$) Cd immobilization capacities compared to the uninoculated control across all metal concentrations evaluated (Table 7). The reference strain CHA0 demonstrated the highest overall immobilization index (88.36%), effectively reducing free Cd in solution to 3.10 mg L^{-1} under acute toxicity conditions (24 mg L^{-1}). Among the autochthonous isolates, T-CADM-5, T-CADE-7, and T-CADE-3 were the most efficient, achieving immobilization indices of 82.41%, 80.14%, and 73.57%, respectively. At the maximum Cd concentration, T-CADM-5 and T-CADE-7 restricted soluble Cd to 6.45 and 6.35 mg L^{-1}, underscoring their robust biosorption and bioprecipitation capabilities. Ureolytic activity drives the generation of HCO_3^-, which interacts with Cd to form the intermediate species Cd-bicarbonate ($CdHCO_3^+$). This biochemical modulation subsequently drives a thermodynamic shift toward CO_3^{2-} saturation, facilitating the precipitation of Cd into the stable mineral phase otavite ($CdCO_3$), significantly limits Cd bioavailability and trophic transfer in contaminated agricultural soils (Bhattacharya et al., 2018; Ma et al., 2023).

Table 7. Evaluation of the Cd immobilization efficiency of autochthonous Cd-tolerant rhizobacteria. Values are mean ± SD (n = 3). Means with similar letters within the same column do not show significant differences ($P \leq 0.05$) by Tukey's multiple comparison test.

	Concentration of Cd (mg L^{-1})				Immobilization
Treatments	0	6	12	24	index (Cd) %
T-CADM-1	0.00 ± 0.00^{a}	4.44 ± 0.40^{c}	5.96 ± 0.59^{bc}	7.31 ± 7.03^{ab}	57.57
T-CADM-4	0.00 ± 0.00^{a}	0.45 ± 0.18^{a}	1.19 ± 0.50^{a}	12.72 ± 5.74^{bc}	65.60
T-CADM-5	0.00 ± 0.00^{a}	0.36 ± 0.18^{a}	0.53 ± 0.11^{a}	6.45 ± 0.38^{ab}	82.41
T-CADM-6	0.00 ± 0.00^{a}	4.05 ± 1.00^{bc}	0.99 ± 0.17^{a}	8.26 ± 0.97^{ab}	68.14
T-CADTC-3	0.00 ± 0.00^{a}	5.38 ± 0.12^{cd}	4.23 ± 0.47^{b}	18.15 ± 0.63^{cd}	33.49
T-CADTC-4	0.00 ± 0.00^{a}	2.71 ± 0.73^{b}	7.51 ± 1.13^{c}	13.93 ± 0.43^{bc}	42.14
T-CADTC-5	0.00 ± 0.00^{a}	4.67 ± 0.23^{cd}	6.97 ± 0.44^{c}	13.53 ± 1.32^{bc}	39.70
T-CADTC-8	0.00 ± 0.00^{a}	4.31 ± 0.15^{c}	9.51 ± 0.18^{d}	25.37 ± 1.84^{d}	6.11
T-CADE-2	0.00 ± 0.00^{a}	4.96 ± 0.40^{cd}	11.40 ± 0.73^{e}	19.06 ± 2.62^{cd}	15.14
T-CADE-3	0.00 ± 0.00^{a}	0.64 ± 0.03^{a}	1.15 ± 1.13^{a}	9.24 ± 3.81^{ab}	73.57
T-CADE-7	0.00 ± 0.00^{a}	0.58 ± 0.07^{a}	1.36 ± 2.00^{a}	6.35 ± 2.68^{ab}	80.14
T-CADE-10	0.00 ± 0.00^{a}	4.42 ± 1.11^{c}	4.84 ± 0.43^{b}	14.14 ± 0.34^{bc}	43.94
CHA0	0.00 ± 0.00^{a}	0.60 ± 0.16^{a}	1.16 ± 0.20^{a}	3.10 ± 0.19^{a}	88.36
Control without bacteria	0.00 ± 0.00^{a}	6.00 ± 0.18^{d}	11.87 ± 0.02^{e}	23.87 ± 0.02^{d}	0.00

Pearson correlation analysis

Pearson correlation analysis (Table 8) revealed a highly significant relationship ($P < 0.001$) between the Cd immobilization index and the percentage increase of HCO_3^- ($r = 0.82$) and SO_4^{2-} ($r = 0.63$). While rhizobacterial biomass (CFU) correlated positively with HCO_3^- production ($r = 0.56$), it did not directly determine overall immobilization. These quantitative links confirm that specific ureolytic and S-oxidizing metabolic pathways—rather than mere population size—are the primary biochemical drivers of Cd biomineralization (Ma et al., 2023; Ranadev et al., 2023).

Table 8. Pearson correlation matrix for each analyzed variable. Highly significant correlations ($p < 0.001$) are shown in bold ($n = 39$). ^{NS}Nonsignificant. CFU: Colony forming units.

Variables	Mean CFU	Increase HCO_3^-	Increase SO_4^{2-}
	mL^{-1}	%	%
Increase HCO_3^-, %	0.56		
Increase SO_4^{2-}, %	^{NS}	0.56	
Immobilization index (Cd), %	^{NS}	0.82	0.63

Molecular identification and phylogenetic analysis based on the 16S rRNA gene

Taxonomic identification categorized the elite autochthonous CdtrB with PGPR functional traits into the *Enterobacter* and *Serratia* genera, with NCBI GenBank identities ranging from 86% to 98% (Table 9). Functional profiling confirmed robust metabolic versatility; all isolates exhibited urease activity and the capacity to precipitate HCO_3^- and SO_4^{2-}, supporting their role in mineral-phase Cd sequestration (Bravo and Braissant, 2022; Ma et al., 2023). Additionally, all strains demonstrated phosphate solubilization, while T-CADM-1 and T-CADM-6 shared the full functional profile of the PGPR strain CHA0, including biofilm formation and protease production (Chávez-Arteaga et al., 2018; Pal and Sengupta, 2019). Resistance to ampicillin was widespread, except in T-CADM-5, which showed the highest susceptibility. These multifaceted traits consolidate the potential of the T-CADM cohort to sustain metabolic activity and drive assisted bioremediation in heavy metal-impacted cacao soils.

Table 9. Taxonomic identification and functional profiling of elite autochthonous Cd-tolerant rhizobacteria compared against the NCBI GenBank database. UR: Urease; BF: biofilm; PS: phosphate solubilization; PR: protease; HCO_3^-: bicarbonate precipitation; SO_4^{2-}: sulfate precipitation; CL: chloramphenicol; AP: ampicillin; S: susceptibility; R: resistance; (+): presence; (-): absence.

	Enzymes			Antagonistic metabolite	Ability to precipitate		Antibiotics		Identity to NCBI GenBank database			
Strains	UR	BF	PS	PR	HCO_3-	SO_4^{2-}	CL	AP	Body	Strain	Identity (%)	Accession number
T-CADM-1	+	+	+	+	+	+	S	R	*Enterobacter* sp.	BAB-5830	86	KX181394.1
T-CADM-4	+	-	+	-	+	+	R	R	*Serratia marcescens*	KC034	98	CP053927.1
T-CADM-5	+	-	+	-	+	+	S	S	*Enterobacter asburiae*	KNUC5007	92	JQ682630.1
T-CADM-6	+	+	+	+	+	+	S	R	*Enterobacter hormaechei*	AMS-38	98	CP051132.1
Control	+	+	+	+	+	+	R	R	*Pseudomonas protegens*	CHA0	100	NR_114749.1

Phylogenetic analysis of 16S rRNA sequences grouped (Figure 6) the elite CdtrB with PGPR functional traits into three highly supported clades (bootstrap ≥ 79%). Isolates T-CADM-4 and T-CADM-5 clustered within Clade I (homologous to *Serratia* and *Enterobacter*), whereas T-CDM-1 and T-CDM-6 formed a divergent monophyletic lineage in Clade III. This distinct evolutionary clustering highlights broad genetic diversity and structural adaptation to heavy metal stress, confirming the robust suitability of these CdtrB for in situ bioremediation and plant growth promotion in Cd-contaminated agroecosystems (Bravo et al., 2018; Huang et al., 2026).

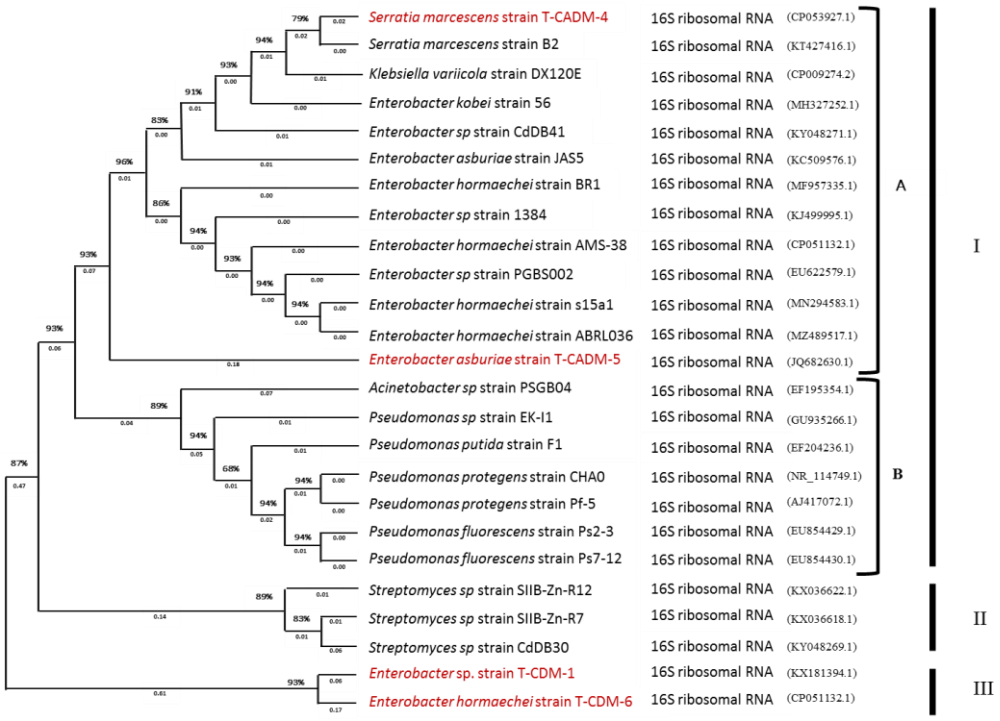

Figure 6. Phylogenetic tree of Cd-tolerant rhizobacteria with plant growth-promoting rhizobacteria functional traits isolates based on 16S rRNA. The tree was constructed using the Neighbor-joining method; evolutionary distances were based on the Kimura 2-parameter model. Horizontal distances are proportional to phylogenetic distances, expressed as substitutions for a bootstrap percentage of 1000 replicates.

CONCLUSIONS

Autochthonous rhizobacteria strains T-CADM1, T-CADM4, T-CADM5, and T-CADM6 demonstrated robust viability under Cd stress, exhibited high capacity to immobilize Cd, with rates higher than 50%, and an efficiency that reached up to 82.41% in the strain T-CADM-5. In addition, these strains produced urease and phosphatase, and show a high production of HCO_3^- and sulfate SO_4^{2-}. The strong positive correlation between HCO_3^- production and the Cd immobilization index (r = 0.82) indicating that these rhizobacteria actively modify their environment to reduce the bioavailability of the heavy metal. Consequently, the strategic assembly of these elite Cd-tolerant rhizobacteria strains with plant growth-promoting rhizobacteria functional traits, in the form of consortia, represents a sophisticated biotechnological frontier for modulating geochemical microenvironments and ensuring metal mitigation in tropical agroecosystems of *Theobroma cacao* L.

Author contribution

Conceptualization: H.F.C., M.C., J.A. Methodology: H.F.C., M.C. Software: J.A., H.F.C. Validation: M.C., H.F.C., J.A. Formal analysis: H.F.C., J.A. Investigation: H.F.C., J.A., L.V., W.D., K.P. Resources: M.C., H.F.C., J.A. Data curation: W.D., L.V., J.A. Writing original draft preparation: H.F.C., J.A. Writing review and editing: J.A., H.F.C., M.C. Visualization: M.C., H.F.C., J.A. Supervision: K.P., L.V., W.D. Project administration: H.F.C., M.C. Funding acquisition: M.C., H.F.C., J.A. All co-authors reviewed the final version and approved the manuscript before submission.

Acknowledgements

The authors express their deep gratitude to the Competitive Fund for Scientific and Technological Research (FOCICYT-9) of the Quevedo State Technical University (UTEQ) for the primary funding of this research. We also acknowledge the technical and logistical support provided by the Department of Soil and Water Management of the National Institute of Agricultural Research (INIAP-EETP, Ecuador) and the support of the Deutsche Gesellschaft für Internationale Zusammenarbeit (GIZ).

References

Abdollahi, S., Golchin, A., Shahryari, F. 2020. Lead and cadmium-resistant bacterial species isolated from heavy metal-contaminated soils show plant growth-promoting traits. International Microbiology 23:625-640. doi:10.1007/s10123-020-00133-1.

Adkin, P., Smith, L.J., Walsh, S.E. 2022. Priming with biocides: A pathway to antibiotic resistance. Journal of Applied Microbiology 133(2):830-841. doi:10.1111/jam.15564.

Andersen, M.A. 2019. Calculating and interpreting percentage changes for economic analysis. Applied Economics Teaching Resources 1(1):25-31.

Argüello, D., Chavez, E., Lauryssen, F., Vanderschueren, R., Smolders, E., Montalvo, D. 2019. Soil properties and agronomic factors affecting cadmium concentrations in cacao beans: A nationwide survey in Ecuador. Science of the Total Environment 649:120-127. doi:10.1016/j.scitotenv.2018.08.292.

Azatian, S.B., Kaur, N., Latham, M.P. 2019. Increasing the buffering capacity of minimal media leads to higher protein yield. Journal of Biomolecular NMR 73(1-2):11-17. doi:10.1007/s10858-018-00222-4.

Bensidhoum, L., Nabti, E., Tabli, N., Kupferschmied, P., Weiss, A., Rothballer, M., et al. 2016. Heavy metal tolerant *Pseudomonas protegens* isolates from agricultural well water in northeastern Algeria with plant growth promoting, insecticidal and antifungal activities. European Journal of Soil Biology 75:38-46. doi:10.1016/j.ejsobi.2016.04.006.

Bhattacharya, A., Naik, S.N., Khare, S.K. 2018. Harnessing the bio-mineralization ability of urease producing *Serratia marcescens* and *Enterobacter cloacae* EMB19 for remediation of heavy metal cadmium (II). Journal of Environmental Management 215:143-152. doi:10.1016/j.jenvman.2018.03.055.

Bravo, D., Braissant, O. 2022. Cadmium-tolerant bacteria: Current trends and applications in agriculture. Letters in Applied Microbiology 74(3):311-333. doi:10.1111/lam.13594.

Bravo, D., Pardo-Díaz, S., Benavides-Erazo, J., Rengifo-Estrada, G., Braissant, O., Leon-Moreno, C. 2018. Cadmium and cadmium-tolerant soil bacteria in cacao crops from northeastern Colombia. International Journal of Laboratory Hematology 38(1):42-49. doi:10.1111/ijlh.12426.

Canchignia-Martínez, H.F., Vera-Benites, L.F., Tapia-Quintana, D.N., Cedeño-Moreira, Á.V., García-Intriago, E., Macías-Holguín, C.J. 2024. Caracterización bioquímica de rizobacterias endófitas con actividad biocontroladora contra *Phytophthora palmivora* y *Lasiodiplodia theobromae*. Terra Latinoamericana 42:e1807. doi:10.28940/terra.v42i0.1807.

Chávez-Arteaga, K.T., Guato-Molina, J.J., Peñafiel-Jaramillo, M.F., Mestanza-Uquillas, C.A., Canchignia-Martínez, H.F. 2018. Bacterias fluorescentes productoras de metabolitos antagónicos de cultivares nativos de *Musa* sp. y su diversidad filogenética al gen ARNr 16S. Ciencia y Tecnología 11(2):17-29. doi:10.18779/cyt.v11i2.204.

Chen, L., Li, K., Shang, J., Wu, Y., Chen, T., Wanyan, Y., et al. 2021. Plant growth – promoting bacteria improve maize growth through reshaping the rhizobacterial community in low-nitrogen and low-phosphorus soil. Biology and Fertility of Soils 57:1075-1088. doi:10.1007/s00374-021-01598-6.

Chompa, S.S., Zuan, A.T.K., Amin, A.M., Hun, T.G., Ghazali, A.H.A., Sadeq, B.M., et al. 2024. Identificación molecular y efecto de rizobacterias promotoras del crecimiento vegetal tolerantes a la sal en el aspecto bioquímico y el crecimiento del arroz. Chilean Journal of Agricultural Research 84:606-619. doi:10.4067/S0718-58392024000500606.

Das, S., Dash, H.R., Chakraborty, J. 2016. Genetic basis and importance of metal resistant genes in bacteria for bioremediation of contaminated environments with toxic metal pollutants. Applied Microbiology and Biotechnology 100(7):2967-2984. doi:10.1007/s00253-016-7364-4.

Dhami, N.K., Mukherjee, A., Reddy, M.S. 2016. Micrographical, minerological and nano-mechanical characterisation of microbial carbonates from urease and carbonic anhydrase producing bacteria. Ecological Engineering 94:443-454. doi:10.1016/j.ecoleng.2016.06.013.

Feria-Cáceres, P.F., Penagos-Velez, L., Moreno-Herrera, C.X. 2022. Tolerance and cadmium (Cd) immobilization by native bacteria isolated in cocoa soils with increased metal content. Microbiology Research 13(3):556-573. doi:10.3390/microbiolres13030039.

Giri, A., Pant, D. 2019. CO_2 management using carbonic anhydrase producing microbes from western Indian Himalaya. Bioresource Technology Reports 8:100320. doi:10.1016/j.biteb.2019.100320.

Gupta, P., Diwan, B. 2017. Bacterial exopolysaccharide mediated heavy metal removal: A review on biosynthesis, mechanism and remediation strategies. Biotechnology Reports 13:58-71. doi:10.1016/j.btre.2016.12.006.

Huang, X., Xu, Z., Gan, L., Wu, R., Huang, Y., Zhang, X., et al. 2026. Insight into the mechanisms of Cd(II) on significantly enhancing rhizobacterial ACC deaminase activity in Cd-tolerant *Ensifer morelensis* A23T. BMC Microbiology 26:274. doi:10.1186/s12866-025-04614-z.

Koua, S.H., N'golo, D.C., Alloue-Boraud, W.M., Konan, F., Dje, K.M. 2020. *Bacillus subtilis* strains isolated from cocoa trees (*Theobroma cacao* L.) rhizosphere for their use as potential plant growth promoting rhizobacteria in Côte d'Ivoire. Current Microbiology 77(9):2258-2264. doi:10.1007/s00284-020-02027-x.

Lee, J., Id, H.K., Jo, H.Y., Jae, M., Id, K. 2021. Revisiting soil bacterial counting methods: Optimal soil storage and pretreatment methods and comparison of culture- dependent and -independent methods. PLOS ONE 16(2):e0246142. doi:10.1371/journal.pone.0246142.

Ma, B., Song, W., Zhang, X., Chen, M., Li, J., Yang, X., et al. 2023. Potential application of novel cadmium-tolerant bacteria in bioremediation of Cd-contaminated soil. Ecotoxicology and Environmental Safety 255:114766. doi:10.1016/j.ecoenv.2023.114766.

Nasser, K., Fonseca, M., Fernando, R., Cristina, E., Vendruscolo, G. 2024. Bacterial quantification in different plating methodologies. Journal of Advances in Biology & Biotechnology 27(8):964-973.

Ntsoli, P.G., Kouam, I.D., Titti, R.W., Marius, G., Kossi, E., Mouthe, D.B., et al. 2025. Yield, production losses, fertility status, and soil microbial population in three different cocoa (*Theobroma cacao* L.) -based cropping systems in an Oxisol in Southern Cameroon. International Journal of Agronomy 2025:8888362. doi:10.1155/ioa/8888362.

Pal, A.K., Sengupta, C. 2019. Isolation of cadmium and lead tolerant plant growth promoting rhizobacteria: *Lysinibacillus varians* and *Pseudomonas putida* from Indian agricultural soil. Soil and Sediment Contamination 28(7):601-629. doi:10.1080/15320383.2019.1637398.

Park, J.H., Bolan, N., Megharaj, M., Naidu, R. 2011. Isolation of phosphate solubilizing bacteria and their potential for lead immobilization in soil. Journal of Hazardous Materials 185(2-3):829-836. doi:10.1016/j.jhazmat.2010.09.095.

Peñafiel, M., Torres, E., Barrera, A., Prieto, H., Morante, J., Canchignia-Martínez, H.F. 2016. Producción de ácido indol-3-acético por *Pseudomonas veronii* R4 y formación de raíces en hojas de vid "Thompson seedless" in vitro. Ciencia y Tecnología 9(1):31-36.

Rana, K., Rana, N., Singh, B. 2020. Applications of sulfur oxidizing bacteria. p. 131-136. In Salwan, R., Sharma, V. (eds.) Physiological and biotechnological aspects of extremophiles. Academic Press, Cambridge, Massachusetts, USA. doi:10.1016/B978-0-12-818322-9.00010-1.

Ranadev, P., Ashwin, R., Bagyaraj, D.J., Shinde, A. 2023. Sulfur oxidizing bacteria in agro ecosystem and its role in plant productivity—a review. Journal of Applied Microbiology 134(8):lxad161. doi:10.1093/jambio/lxad161.

Renu, S., Sarim, K.M., Singh, D.P., Sahu, U., Bhoyar, M.S., Sahu, A., et al. 2022. Deciphering cadmium (Cd) tolerance in newly isolated bacterial strain, *Ochrobactrum intermedium* BB12, and its role in alleviation of Cd stress in spinach plant (*Spinacia oleracea* L.) Frontiers in Microbiology 12:758144. doi:10.3389/fmicb.2021.758144.

Sheikhi, S., Shahbazi, H., Mosaferi, M., Firuzi, P., Aslani, H. 2020. Spatio-temporal variation of WQI, scaling and corrosion indices, and principal component analysis in rural areas of Marand, Iran. Groundwater for Sustainable Development 11:100480. doi:10.1016/j.gsd.2020.100480.

Stamenov, D., Jafari, T.H., Djuric, S., Kiprovski, B., Acimovic, M. 2024. Mitigating effect of PGPR on abiotic stress in basil (*Ocimum basilicum* L.) Chilean Journal of Agricultural Research 84:588-596. doi:10.4067/S0718-58392024000500588.

Ultanbekova, G., Jumakhanov, B., Nussupov, A., Faleev, D. 2025. The role of *Bacillus megaterium* PEF-1 in stimulating the growth of organic cotton under environmental stress conditions. Scientific Reports 15:45729.

Wang, T., Wang, S., Tang, X., Fan, X., Yang, S., Yao, L., et al. 2020. Isolation of urease-producing bacteria and their effects on reducing Cd and Pb accumulation in lettuce (*Lactuca sativa* L.) Environmental Science and Pollution Research 27(8):8707-8718. doi:10.1007/s11356-019-06957-3.